



DESIGN EQUATIONS FOR DEFORMATION CAPACITY OF REINFORCED CONCRETE COLUMNS FAILING IN FLEXURE

Eiichi INAI¹ and Hisahiro HIRAISHI²

SUMMARY

Reinforced concrete columns subjected to shear and high axial forces typically fail due to the crush of concrete after flexural yielding. In this paper, the design equations for the deformation capacity of these columns, which have been proposed in the authors' previous paper, are examined using the experimental data with a very wide range of structural parameters. It is concluded that the design equations give a lower boundary of experimental data, and that they are useful to predict the deformation capacity of the columns subjected to a varying axial force as well as a constant axial force.

INTRODUCTION

Deformation capacity after flexural yielding of reinforced concrete columns depends on the mechanical characteristic of core concrete in the hinging region at the column end, as well as the axial load. Through the experimental and theoretical investigations on the mechanical characteristic of core concrete, two criteria determining the deformation capacity of the columns have been clarified by Hiraishi [1], Hiraishi [2] and Inai [3]. One is the deformation capacity under monotonic lateral loading, which is caused by the strain softening of core concrete. The other is the deformation capacity due to cyclic lateral loading, which is caused by the hysteretic behavior of core concrete. These deformation capacities have been theoretically investigated and formulated as relationships between the axial stress ratio and the ultimate curvatures by Hiraishi [4]. Based on these theoretical relationships, design equations for the ultimate drift angle of the columns under a constant axial load have been proposed by Inai [5]. Furthermore, these design equations have been extended for the columns subjected to not only a constant axial force but also a varying axial force by Inai [6]. In this paper, the proposed design equations are examined by the experimental data with a very wide range of structural parameters

DESIGN EQUATIONS FOR DEFORMATION CAPACITY

The ultimate drift angle of the columns proposed by Inai [6] is determined by the smaller one between the ultimate drift angle under monotonic lateral loading R_{u1} and the ultimate drift angle due to cyclic lateral loading R_{u2} . R_{u1} is expressed by Eq. (1) as a function of η_m . R_{u2} is expressed by Eq. (2) as a function of η_{eq} . These relationships are shown in Fig. 1.

¹ Associate Professor, Yamaguchi University, Ube, Japan, Email: inai@yamaguchi-u.ac.jp

² Professor, Meiji University, Kawasaki, Japan, Email: hiraishi@isc.meiji.ac.jp

$$R_{u1} = (1 - \eta_m) / 24 \quad \text{for } R_{u1} \leq 1/34 \quad (1a)$$

$$R_{u1} = (1 - 2 \cdot \eta_m) / 14 \quad \text{for } 1/34 \leq R_{u1} \leq 0.06 \quad (1b)$$

$$R_{u2} = (1 - \eta_{eq}) / 57 \quad \text{for } R_{u2} \leq 0.01 \quad (2a)$$

$$R_{u2} = (1 - 2 \cdot \eta_{eq}) / 14 \quad \text{for } 0.01 \leq R_{u2} \leq 0.06 \quad (2b)$$

$$\text{where } \eta_m = (\eta_L + \eta_{E+}) - \eta_{SY} \quad (3)$$

$$\eta_{eq} = \eta_L + 1/2 \cdot \eta_{E+} - 1/3 \cdot \eta_{E-} - 1/3 \cdot (\eta_{S++} + \eta_{S-} + \eta_{S^0}) \quad (4)$$

$$\eta_L = N_L / (A_c \cdot f'c)$$

$$\eta_{E+} = N_{E+} / (A_c \cdot f'c)$$

$$\eta_{E-} = N_{E-} / (A_c \cdot f'c)$$

$$\eta_{SY} = 1/2 \cdot (\sum a_{cs} \cdot \sigma_{cy}) / (A_c \cdot f'c) \quad (5)$$

Values of η_{S+} , η_{S-} and η_{S^0} are as follows.

$$\eta_{S+} = \eta_L + \eta_{E+} \quad \text{for } \eta_L + \eta_{E+} < \eta_{SY}, \quad \eta_{S+} = \eta_{SY} \quad \text{for } \eta_L + \eta_{E+} \geq \eta_{SY}$$

$$\eta_{S-} = \eta_L - \eta_{E-} \quad \text{for } \eta_L - \eta_{E-} < \eta_{SY}, \quad \eta_{S-} = \eta_{SY} \quad \text{for } \eta_L - \eta_{E-} \geq \eta_{SY}$$

$$\eta_{S^0} = \eta_L + 1/2 \cdot \eta_{E+} \quad \text{for } \eta_L + 1/2 \cdot \eta_{E+} < \eta_{SY}, \quad \eta_{S^0} = \eta_{SY} \quad \text{for } \eta_L + 1/2 \cdot \eta_{E+} \geq \eta_{SY}$$

where η_m = the axial stress ratio of concrete at the maximum compressive axial load; η_{eq} = the axial stress ratio of concrete considering the variation of axial load; N_L = the long-term axial load (positive value for compression); N_{E+} = the earthquake-induced compressive axial load (positive value for compression); N_{E-} = the earthquake-induced tensile axial load (positive value for tension); A_c = the area of core section ($b' \times D'$ in Fig. 2); $f'c$ = the compressive strength of core concrete; a_{cs} = the area of longitudinal reinforcing bars in the central area at column section (inner reinforcing bars and outer reinforcing bars in the hatched area shown in Fig. 2); σ_{cy} = the yield strength of the above reinforcing bars.

In case of the columns subjected to a constant axial force, R_{u2} becomes equal to or smaller than R_{u1} as illustrated in Fig. 1 because η_m is equal to η_{eq} . Therefore, it is enough for determining the ultimate drift angle to use Eq. (2). However, in case of the exterior columns subjected to a large earthquake-induced axial force, there is a possibility that the deformation capacity is determined by R_{u1} on the lateral loading

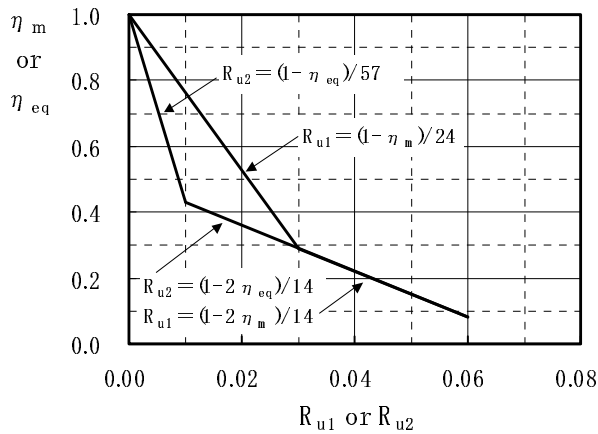


Fig. 1 $\eta_m - R_{u1}$ and $\eta_{eq} - R_{u2}$ relationships

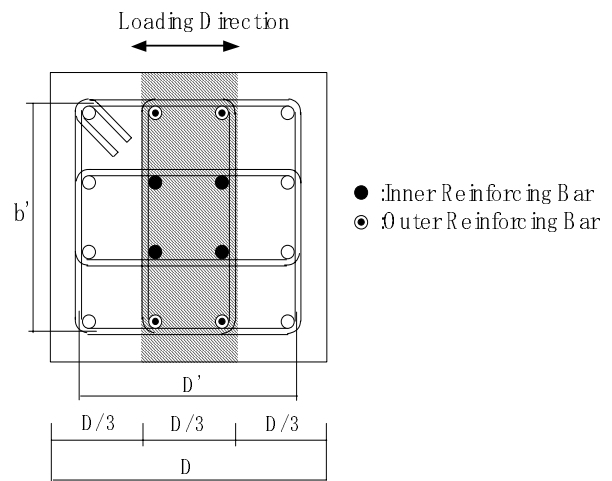


Fig. 2 Definition of central area at section

side under a high axial compression before it is determined by R_{u2} . This is because the core concrete sustains little damage while the axial load is small compression or tension even if the column is subjected to the lateral cyclic loading. Therefore, it is necessary to compare the two values obtained by Eq. (1) and Eq. (2) for determining the ultimate drift angle.

Figure 3 gives relationships between the axial stress ratio $N/(b'D'f_c)$ and the normalized ultimate curvatures, $\phi_{SL}D'/\epsilon_B$ and $\phi_{CY}D'/\epsilon_B$, of a doubly reinforced concrete core section without reinforcing bars in the central area subjected to a constant axial force, which have been theoretically formulated by Hiraishi [4]. These relationships were obtained from the simplified stress-strain relationship for core concrete as illustrated in Fig. 4. In Figs. 3 and 4, N = a constant axial load; D' and b' = depth and width of core section; ϵ_B = the strain at the compressive strength of core concrete; α = a parameter representing the slope of descending branch of stress-strain relationship of core concrete; ϕ_{SL} = the ultimate curvature under monotonic lateral loading; ϕ_{CY} = the ultimate curvature due to cyclic lateral loading. The two normalized ultimate curvatures reduce as the value of α becomes large, in particular the normalized ultimate curvature under monotonic lateral loading. The value of ϕ_{SL} is very sensitive to α . Matsuura [7] investigated the slope of descending branch of core concrete using the test results of centrally loaded column specimens in the existing literatures, and obtained a correlation between the value of α and a confinement index C_c given by Eq. (6). Figure 5 indicates that most of the values of α is distributed in the range 0.0 to 0.2 for the column specimens with C_c of more than 0.05.

$$C_c = (1 - 0.5 \cdot S / D')^2 \cdot p_w' \cdot \sigma_{wy} / \sigma_b \quad (6)$$

where S = the spacing of lateral reinforcement ; p_w' = the ratio of lateral reinforcement using core width; σ_{wy} = the yield strength of lateral reinforcement; σ_b = the compressive strength of core concrete without lateral reinforcement ($= 0.85 \sigma_B$); σ_B = the compressive strength of concrete cylinder.

Equation (1) was derived from a relationship between the axial stress ratio and ϕ_{SL} with α of 0.2 and ϵ_B of 0.3 %. Equation (2) was also derived from a relationship between axial stress ratio and ϕ_{CY} with α of 0.2 and ϵ_B of 0.3 %. Equation (7) was used to obtain drift angle of column. The values of 0.2 for α and 0.3% for ϵ_B were determined by Inai [5] expecting that Eqs. (1) and (2) gave lower boundaries of test results of column specimens subjected to axial and shear forces. The axial stress ratios of concrete

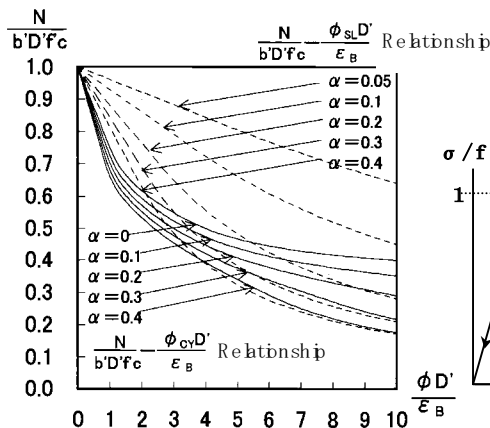


Fig. 3 Ultimate Curvatures under a constant axial load

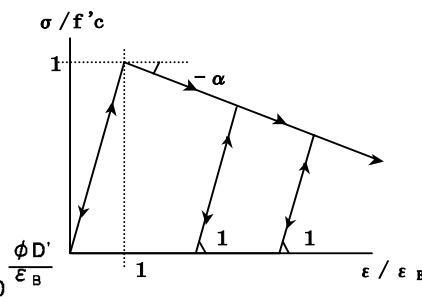


Fig. 4 Simplified stress-strain relationship for core concrete

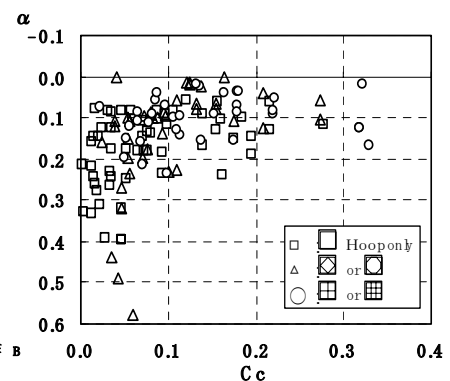


Fig. 5 Distribution of α

expressed by Eqs. (3) and (4) were introduced by Inai [6] in order to represent the effects of the variation of axial load and the presence of longitudinal reinforcing bars in the central area at column section. In the exterior columns of high-rise buildings, the axial load varies to tension due to the overturning moment during severe earthquakes. Such exterior columns usually have inner reinforcing bars in the central area to resist tensile axial load.

$$R = \phi \cdot L_p \tag{7}$$

where R = the drift angle of column; ϕ = the curvature in the hinging region at column end; L_p is a length of the hinging region and is assumed to be D' .

DATABASE ON DEFORMATION CAPACITY

The database used for verifying the proposed design equations mainly consists of test results of the specimens representing the columns of high-rise buildings in the existing literatures listed in Inai [8]. The number of the specimens subjected to a constant axial force and cyclic lateral force is thirty-two. The number of the specimens subjected to a varying axial force and cyclic lateral force is twenty. The dimensions, the material strengths and the amount of reinforcement of the specimens in the database are

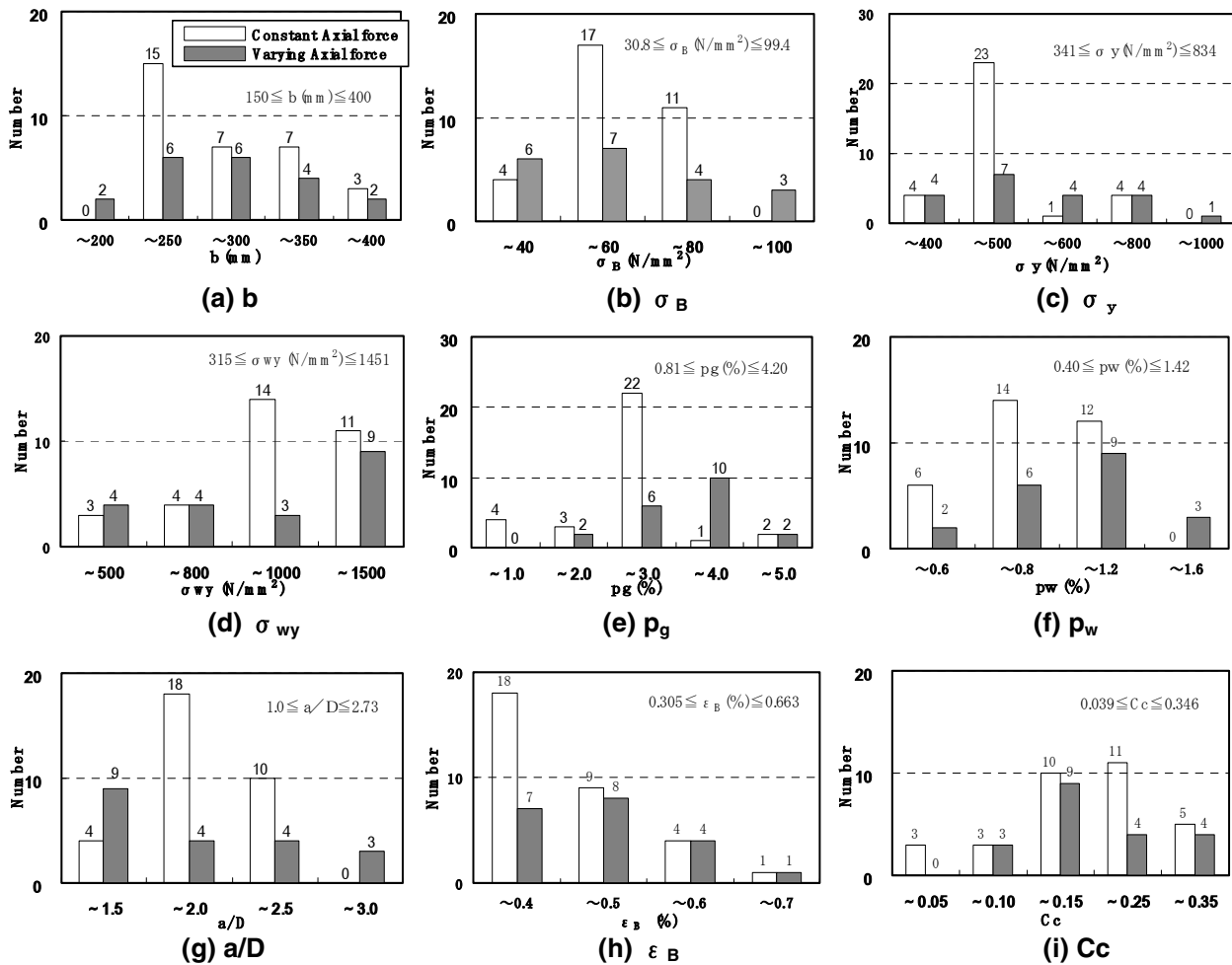


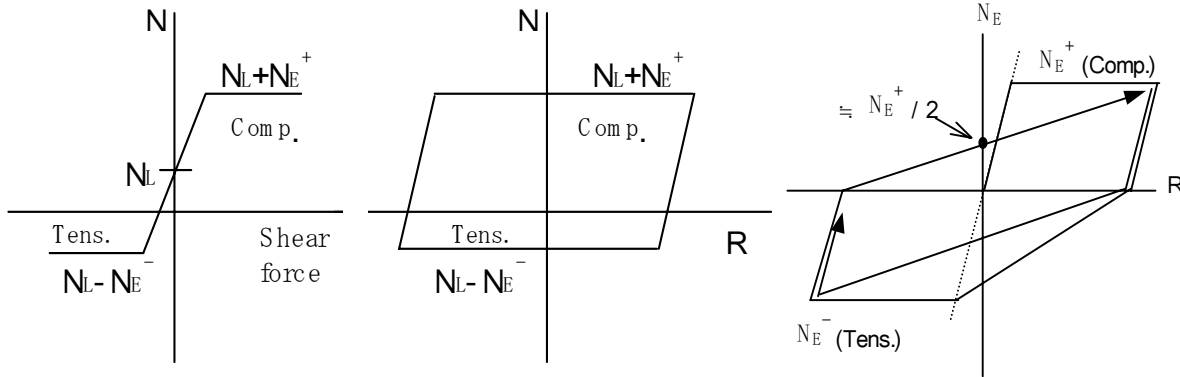
Fig. 6 Structural parameters of column specimens in database

shown in Fig. 6. The column width b is in the range 150 to 400 mm. The concrete strength σ_B is in the range 30.8 to 99.4 N/mm². The yield strength of longitudinal reinforcing bars σ_y is in the range 341 to 834 N/mm². The yield strength of lateral reinforcement σ_{wy} is in the range 315 to 1451 N/mm². The ratio of longitudinal reinforcing bars p_g is in the range 0.81 to 4.20 %. The ratio of lateral reinforcement p_w is in the range 0.40 to 1.42 %. The ratio of shear span to column depth a/D is in the range 1.0 to 2.73. The strain at the compressive strength of core concrete ϵ_B is estimated to be in the range 0.305 to 0.663 %. The minimum value of ϵ_B of specimens in the database is 0.3 %. The confinement index C_c is in the range 0.039 to 0.346. Fig. 6(i) and Fig. 5 indicate that the maximum value of α of the specimens in the database is almost 0.2 except for three specimens with C_c of less than 0.05.

The deformation capacity of the specimens was defined as the drift angle on the envelope curve where the resisting moment reduced to 95 % of the maximum strength. However, the reduction in moment resistance due to the crush of cover concrete was ignored. All of specimens in the database were subjected to the cyclic lateral force. Therefore, the test results of thirty-two specimens subjected to a constant axial force were compared with the ultimate drift angle due to cyclic lateral loading R_{u2} expressed by Eq. (2). In this case, the values of η_{eq} of the specimens were obtained from substituting zero for N_{E+} and N_{E-} in Eq. (4). On the other hand, the test results of fourteen specimens subjected to a varying axial force, which was proportional to the shear force of the column as illustrated in Fig. 7(a), were compared with the ultimate drift angle under monotonic lateral loading R_{u1} expressed by Eq. (1). Inai [6] has pointed out that the axial load in such specimens is large compression only around a peak of the lateral deformation in a loading cycle, while it is relatively small compression or tension in the rest of the loading cycle. As a result, these specimens are considered to have little influence of the cyclic lateral loading. In this case, the values of η_m of the specimens were obtained from substituting the maximum compressive load of the specimen for $(N_L + N_{E+})$ in Eq. (3). Test results of six specimens subjected to a varying axial force, which gave large axial compression to the specimen in half of a loading cycle as illustrated in Fig. 7(b), were compared with the ultimate drift angle due to cyclic lateral loading R_{u2} . The values of η_{eq} of these specimens were obtained from using Eq. (8) instead of Eq. (4).

$$\eta_{eq} = 2/3 \cdot \eta_L + 1/3 \cdot \eta_{E+} - 1/3 \cdot \eta_{E-} + 1/3 \cdot \eta_0 - 1/3 (\eta_{S+} + \eta_{S-} + \eta_{S^0}) \quad (8)$$

where $\eta_0 = N_0 / (A_c f_c)$; N_0 is the axial load at the lateral deformation of zero. Equation (8) is an original of Eq. (4). Equation (4) has been obtained from substituting $(\eta_L + 1/2 \eta_{E+})$ for η_0 in Eq. (8), considering the earthquake-induced axial load as illustrated in Fig. 8. Equation (9) was also used instead of Eq. (5) for estimating the axial load supported by longitudinal reinforcing bars in the central area. Equation (5) was



(a) Varying axial force proportional to shear force
 (b) Varying axial force depending on deformation
 Fig. 7 Type of varying axial force

Fig. 8 Assumed earthquake-induced axial load in Eq. (4)

determined expecting the design equations not to overestimate the axial load supported by the reinforcing bars.

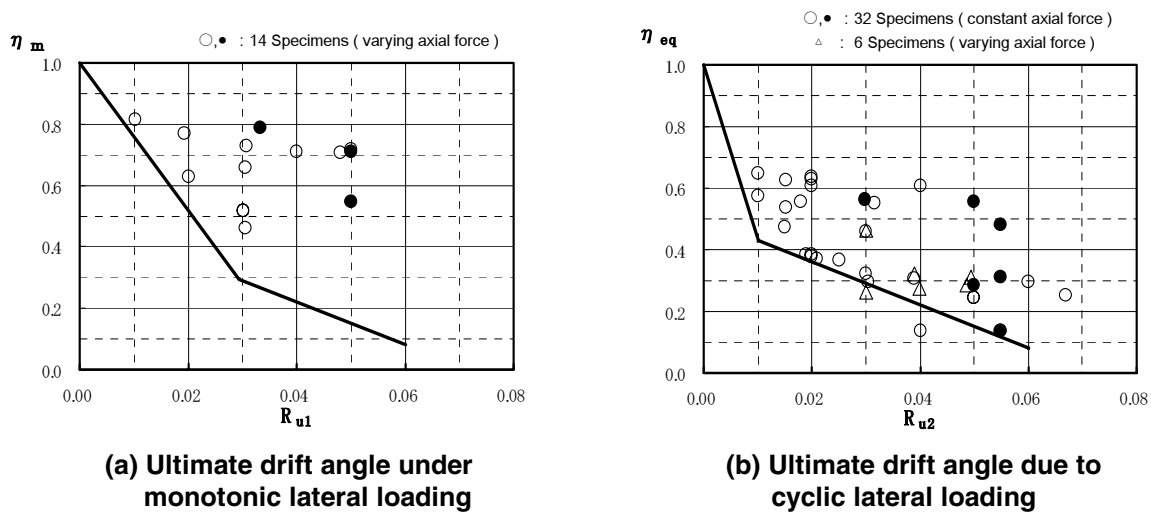
$$\eta_{SY} = (\sum a_{cs} \sigma_{cy}) / (Ac \cdot f'c) \quad (9)$$

The compressive strength of core concrete confined by lateral reinforcement $f'c$ and the strain at the compressive strength of core concrete ϵ_B were estimated by the method proposed by Sakino [9].

VERIFICATION OF DESIGN EQUATIONS

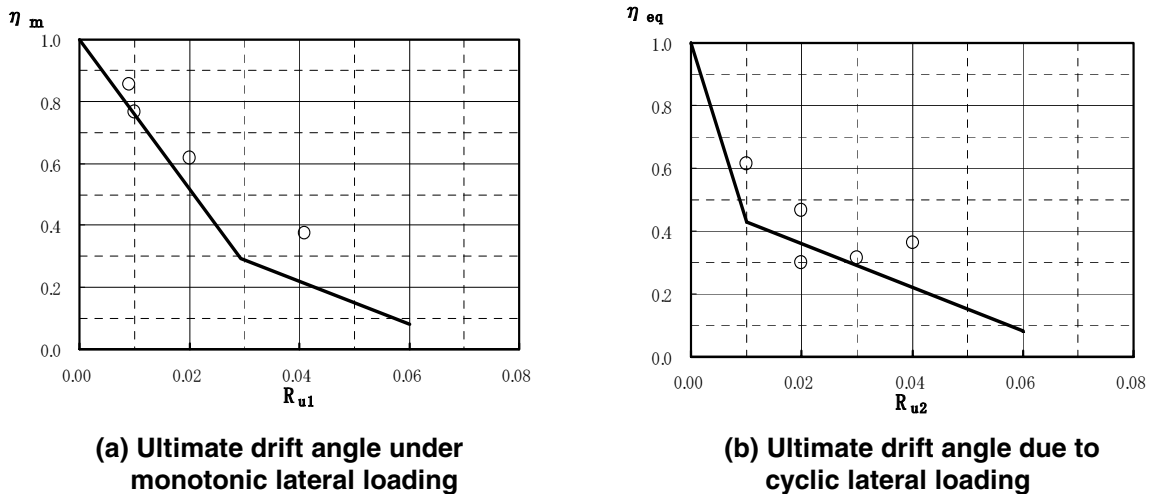
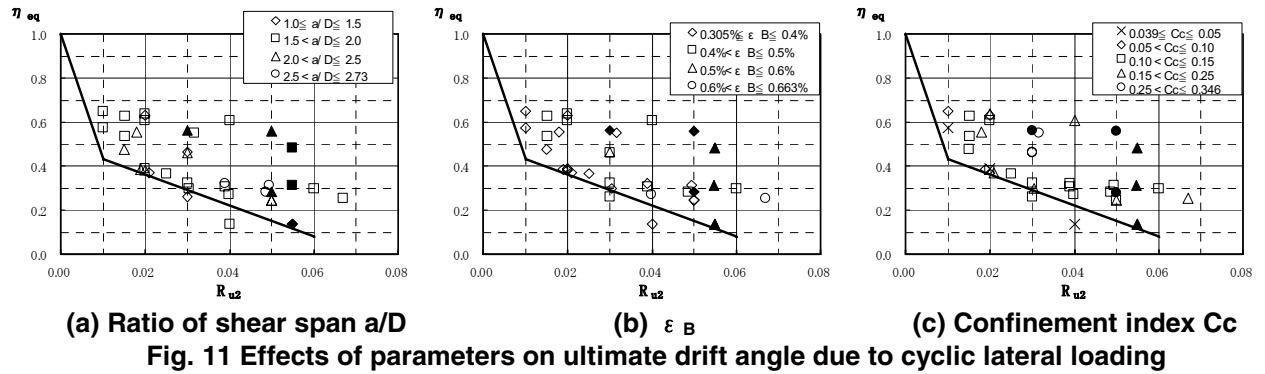
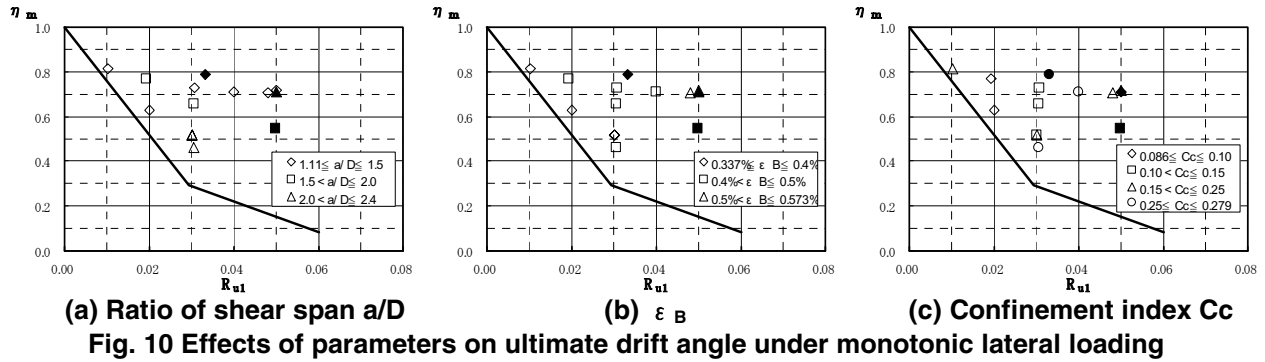
Figure 9(a) gives a comparison between the design equation for R_{u1} and the tests results of fourteen specimens. Figure 9(b) gives a comparison between the design equation for R_{u2} and the tests results of thirty-eight specimens. These figures indicate that the two design equations give a lower boundary of test results respectively. As mentioned above, the design equations have been obtained from using 0.2 as α and 0.3 % as ϵ_B in the ultimate curvatures shown in Fig. 3, and using Eq. (7) in spite of the ratio of shear span a/D . The effects of these parameters, a/D , ϵ_B and α on the ultimate drift angles are shown in Figs. 10 and 11. Figures 10(a) and 11(a) indicate that there is little correlation between the ratio of shear span and the ultimate drift angles. Figures 10(b) and 11(b) indicate that the ultimate drift angles increase as ϵ_B becomes large. Figures 10(c) and 11(c) indicate that the ultimate drift angles increase as Cc becomes large. One of the specimens with Cc of 0.039 has a much smaller ultimate drift angle than that given by the design equation. These indications show that the design equations are adequate.

Recently, behavior of reinforced concrete columns using high-strength materials, including over 100 N/mm² concrete, 685 N/mm² class longitudinal reinforcing bars and 1275 N/mm² class lateral reinforcement, has been investigated in Watanabe [10] and Hatori [11]. Figure 12 gives comparisons between the design equations and test results of the specimens with over 100 N/mm² concrete. The axial stress ratio of concrete and the ultimate drift angles of these specimens were obtained by the same procedure as described above. Figure 12 gives a possibility that the design equations are adaptable for the columns with over 100 N/mm² concrete, however more verifications are needed.



• denotes the maximum experienced drift angle of the specimen with little reduction in resisting moment.

Fig. 9 Comparisons between design equations and test results of specimens in database



CONCLUSIONS

The following conclusions can be drawn from this study.

- 1) The ultimate drift angle under monotonic lateral loading R_{u1} expressed by Eq. (1) gives a lower boundary of test results of the specimens in the database.
- 2) The ultimate drift angle due to cyclic lateral loading R_{u2} expressed by Eq. (2) gives a lower boundary of test results of the specimens in the database.

- 3) The effects of structural parameters on the experimental ultimate drift angle indicate that the design equations are adequate.
- 4) There is a possibility that the design equations are adaptable for the columns with over 100 N/mm^2 concrete.

REFERENCES

1. Hiraishi H., Inai E. "Theoretical study on the deformation capacity of R/C columns beyond flexural yielding." *Journal of Structural and Construction Engineering of AIJ (Architectural Institute of Japan)*, 1990, No.408, 21-30.
2. Hiraishi H., Inai E., et al "Deformation capacity beyond flexural yielding of reinforced concrete columns, part 1 compression tests, bending tests and shear bending tests of columns, and their correlation." *Journal of Structural and Construction Engineering of AIJ*, 1990, No.410, 27-39.
3. Inai E., Hiraishi H. "Deformation capacity beyond flexural yielding of reinforced concrete columns, part 2 stable limit and quasi-stable limit." *Journal of Structural and Construction Engineering of AIJ*, 1992, No.440, 67-76.
4. Hiraishi H., Inai E., Yagenji A. "Deformation capacity of reinforced concrete columns under cyclic loadings, deformation capacity beyond flexural yielding of reinforced concrete columns, part 3." *Journal of Structural and Construction Engineering of AIJ*, 1993, No.454, 127-138.
5. Inai E., Hiraishi H., Yagenji A. "Design equations for deformation capacity of reinforced concrete columns failing in flexure under a constant axial load." *Journal of Structural and Construction Engineering of AIJ*, 2000, No.536, 129-134.
6. Inai E., Hiraishi H. "Deformation capacity of reinforced concrete columns failing in flexure considering variation of axial load and design equations." *Journal of Structural and Construction Engineering of AIJ*, 2001, No.545, 119-126.
7. Matsuura T., Yagenji A. "Review of experimental studies on RC columns subjected to uniaxial compressive load." *Summaries of Technical Papers of Annual Meeting, AIJ, Structures II*, 1992, 1005-1006.
8. Inai E., Hiraishi H. "Design Equations for deformation capacity of reinforced concrete columns failing in flexure." *AIJ Journal of Technology and Design*, 2003, No.18, 109-114.
9. Sakino K., Sun Y. "Stress-strain curve of concrete confined by rectilinear hoop." *Journal of Structural and Construction Engineering of AIJ*, 1994, No.461, 95-104.
10. Watanabe H., et al "Structural performance of RC columns using ultra high strength concrete subjected to high axial load." *Summaries of Technical Papers of Annual Meeting, Structures IV, AIJ*, 2003, 151-154.
11. Hatori T., et al "Experimental study on behavior of reinforced concrete columns using high-strength materials." *Summaries of Technical Papers of Annual Meeting, Structures IV, AIJ*, 2003, 155-158.